UNIVERSITY of CALIFORNIA
SANTA CRUZ

EFFECTS OF CLUSTER DYNAMICS ON THE BIRTH ENVIRONMENT OF THE SOLAR SYSTEM

A thesis submitted in partial satisfaction of the
requirements for the degree of

BACHELOR OF SCIENCE

in

PHYSICS

by

Donald A Dukes

6 June 2011

The thesis of Donald A Dukes is approved by:

Assistant Professor Mark Krumholz
Advisor

Adriane Steinacker
Theses Coordinator

Professor David P. Belanger
Chair, Department of Physics

Abstract

Effects of Cluster Dynamics on the Birth Environment of the Solar System

by

Donald A Dukes

We preformed scattering simulations with the Solar System and other stars to simulate the effects a close encounter would have on the Solar System formation while it is still forming within its birth cluster. Our data from the simulations shows that, contrary to prior work, the cluster dynamics within the birth cluster has little effect on the evolution of the Solar System, and that cluster dynamics should not be used in determining the membership size of our birth cluster. Lifting this constraint on the upper bound of the birth cluster membership size then elevates tension between meteoritic evidence and perviously proposed upper bound of the birth cluster membership size. Also, we showed that the Kupier Belt object Sedna and the drastic drop in object density of the Kuiper belt cannot be explained by a close encounter within the birth cluster except in extreme conditions.

Contents

To

my late grandparents,

Don and Pauline Dukes,

may they rest in peace.

Acknowledgements

I want to thank Lindsey Dukes, for her ever present love, support and just being the best pie ever, my parents Chris and Brenda Dukes, for there long years of support in all of my life's works and adventures, and to Mark Krumholz, for his door always being open and his knowledge and patience being vast. I feel lucky being surrounded by such an amazing group of people.

1 Introduction

It is very likely that our Sun wasn't born in an isolated event, but as part of a star cluster. The birth cluster environment is a self-gravitating system of gas and dust that collapses at a multitude of points to create its membership of stars. This process is inefficient, converting only 10% to 30% of the mass to stars while leaving 70% to 90% as gas (Lada and Lada, 2003). As long as the gas remains, the stars are gravitationally bound and orbit chaotically throughout the cluster. This motion continues until the winds and ionizing radiation of the newborn stars blow away the remaining gas. At that point the cluster is no longer self-gravitating, it disperses and the stars are free to move about the galaxy (Adams, 2010; Chandar et al., 2010; Lada and Lada, 2003).

The chaotic motion of stars within the Sun's birth cluster led the Sun to have to close encounters with other stars, which in turn affected the future shape of the Solar System. By examining the state of our Solar System as it exists today, we can put constraints on the birth cluster's properties. This in turn allows us to identify theoretical constraints on what might still be lurking undetected in the far outer Solar System.

Meteorites provide one line of evidence we can use to constrain the birth cluster's properties. The examination of meteorite samples shows daughter products of multiple radioactive isotopes (isotopes, daughter products and half-lives are shown in Table 1.1). These radioactive isotopes most likely originated from stellar nucleosynthesis and their presence suggests that there was a nearby supernova that enriched the Solar Nebula with these isotopes. The evidence of these isotopes comes from meteorites that formed very early in the Solar System's development, indicating that it was

exposed during the period of planet formation. To have such exposure so early would suggest that the birth cluster would have to be able to produce a star of around 25 solar masses or more. In addition to that, the supernova would have to be close enough to deposit the isotopes (< 0.3 pc), yet not so close as to have stripped off the Solar Nebula's mass with the supernova blast (> 0.1 pc). Both of these considerations suggest a large birth cluster. Adams (2010) estimates that it had to have at least 1000 members.

Table 1.1: Radio Isotopes. Taken from Adams (2010)

Nuclear Species	Daughter	Half-life (Myr)
^{7}Be	^{7}Li	53 days
^{10}Be	^{10}B	1.5
^{26}Al	^{26}Mg	0.72
^{36}Cl	^{36}Ar	0.30
^{41}Ca	^{41}K	0.10
^{53}Mn	^{53}Cr	3.7
^{60}Fe	^{60}Ni	1.5
^{107}Pd	^{107}Ag	6.5
^{182}Hf	^{182}W	8.9

An upper bound on the birth cluster size comes from cluster dynamics. Given the chaotic environment of the birth cluster and the lower limit on its membership, close encounters between star systems are to be expected. These close encounters would perturb the Solar Nebula during its formation. Any such perturbation must still permit the formation of a Solar System like the one we see today.

Our Solar System currently has eight well ordered planets. Their orbits all lie close to the same plane (inclination angles $\leq 3.5^{\circ}$), and they have small eccentricities (less than 0.2, or less than 0.09 is we exclude Mercury, whose eccentricity is pumped by perturbations from other planets). This suggests that no star passed closer than 225 AU from the Sun in the epoch after formation of the gas giants (Adams, 2010). By coupling this limit on the closest approach with the observation that clusters take $\sim$ 1-4 crossing times to form (Adams, 2010; Lada and Lada, 2003; Tan and et al., 2006), Adams estimates an upper limit of $\sim 10^4$ stars on the size of the birth cluster.

This upper limit of membership size is in tension with the proposal of a nearby supernova to explain the meteoritic evidence. The lifetime of a 25 $M_\odot$ star before it goes supernova is ~ 7.54 Myr. Lada and Lada (2003) estimates one crossing time to be $\sim$1 Myr, and given that the Solar System should reside within the birth cluster for $\sim 1 - 4$ crossing times, a 25 $M_\odot$ would take too long to evolve to be the cause of the radioactive isotopes. A 75 $M_\odot$ star, however, has a lifetime of ~ 3.64 Myr. According to Adams (2010), to have a reasonable probability of producing such a star, a birth cluster of membership size of $> 10^4$ will be needed.

We can now turn to the main goal of this work: studying the implications of cluster size and cluster dynamics on the Solar System, and the effects of encounters for other birth cluster members on the formation of our outer Solar System and the objects that are likely to be lurking out in the dark. Three areas of particular interest are the abrupt density decline in the Kuiper Belt at 45 AU, the unusal Kuiper Belt Object Sedna, and the hypothesized Nemesis star.

Current understanding of the formation of the Solar System suggests a large population of small bodies left over from the formation epoch should exist outside of Neptune's orbit. This area is known as the Kuiper Belt. The existence of Neptune, with its size and orbit, suggests that the surface density of the Solar Nebula would have been high enough to produce KBOs out to distances much greater than 50 AU, with a gradually declining object density proportional to $\frac{1}{r}$. Neptune's gravitational influence become insignificant beyond 50 AU, which implies that it could not perturb objects outside of this range. Nonetheless, current observations show that there is a abrupt object density decline of the Kuiper Belt at about 45 AU. Three hypotheses have been proposed to explain this: that a close encounter with an impact parameter of less than 90 AU truncated the disk, that objects are there but are dynamically cold, and that Neptune and Uranus formed closer in and migrated out after formation (Allen et al., 2001). However, there has been only limited studies of the first of these possibilities and Adams (2010) estimates from these limited studies that the rate of such close encounters is only $\sim 10^{-3}$ Myr^{-1}.

Close encounters in the Sun's birth cluster could also help explain the Kuiper Belt Object

Sedna. This object has an unusual orbit quite different from that of other Kuiper Belt Objects (KBOs). Its eccentricity is 0.84, and its perihelion is 76 AU (Adams, 2010; Schwamb and et al., 2010). In contrast, other KBOs tend not to have perihelia above 45 AU, and have an average eccentricity of 0.3 (Schwamb and et al., 2010). If the Solar Nebula were left to itself, we would expect it to create well ordered objects orbiting the Sun. This is because collisions between particles within the nebula transfers energy between particles, which tends to average out the velocities of forming objects and produce low eccentricities. For an object like Sedna to have a high eccentricity, more energy would have to have been transferred to it than to other objects nearby. One possible explanation for the existence of Sedna is that there was a close encounter between the Sun and another star that perturbed a KBO's orbit (Adams, 2010). Previous simulations have studied how encounters might affect the gas giants, but very few simulations have been done to study how encounters might affect the Kuiper Belt.

There has also never been a study of the implications of close encounters for the Nemesis Hypothesis. Nemesis was first proposed in 1984 to explain a puzzling 26 million year periodicity in mass extinction in the fossil records on Earth (Raup and Sepkoski Jr., 1984) (See Fig. 1.1). Periodic mass extinctions with such regularity on our planet would seem to suggest an astronomical explanation. Two independent groups of astronomers, Davis et al. (1984) and Whitmire and Jackson IV (1984), put forth as a possible explanation that our Sun has a companion star, which they called Nemesis. They hypothesized that such a star would perturb objects in the Oort Cloud, sending them into the inner Solar System, which would result in a periodic increase in the rate of impact of extraterrestrial objects into the Earth. This would cause mass extinctions.

Both groups have identified limits as to where Nemesis could exist: its semi-major axis would have to be from 33,000 AU to 88,000 AU, and its eccentricity would have to be greater than 0.7. Given the mean semi-major axis of the Oort Cloud objects, ∼30,000 AU (Davis et al., 1984), a companion to the Sun with these orbital parameters could orbit just outside the Oort Cloud, periodically dipping into it. This, in turn, would cause perturbations that would shower the Solar

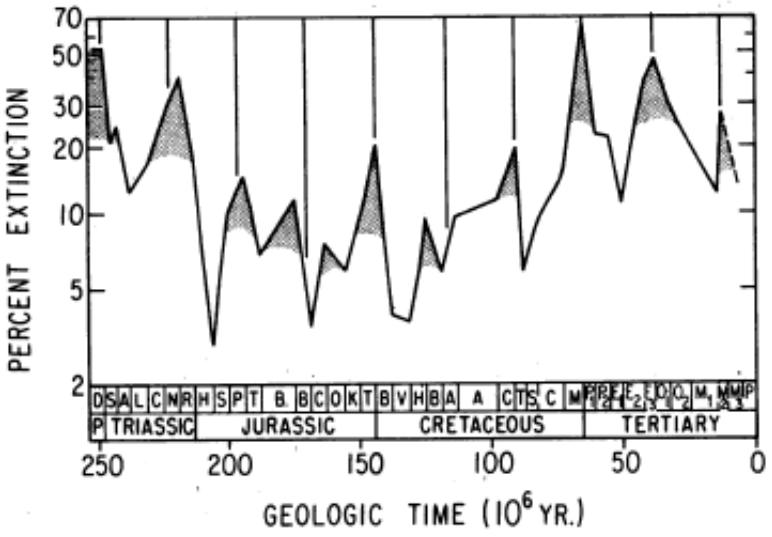

Figure 1.1: Extinction record for the past 250 ma. Letter codes (bottom) identify stratigraphic stages. The best-fit 26-Myr cycle is shown along the top as vertical lines. The relative heights of extinction peaks should not be taken as literal expressions of extinction intensity because the absence of extant taxa exaggerates the heights of younger peaks (Raup and Sepkoski Jr., 1984).

System with Oort Cloud debris. Given the number density of the Oort Cloud and the range of possible Nemesis properties, an estimated 25 to 50 objects would strike the earth every 26 million years under this scenario.

Given that Nemesis has not been observed, Whitemire & Jackson estimate that such an object would have to have a mass below $8 \times 10^{-2}\ M_{\odot}$. Below this mass, an object would not have enough gravitational energy to ignite fission within its core. This would allow Nemesis to remain undetectable in the visible and extremely dim in infrared bands. It would also have a negligible gravitational impact on the the orbits of planets and KBOs. These factors would allow Nemesis to elude detection.

But how would such an object get there? There are two possibilities: either Nemesis was captured after the Solar System was formed, or it formed with Sun. The statical likelihood of the former is extremely low. A formation of a binary system from two unbound stars would require

a three body encounter, so as to shed kinetic energy to the third star. Simulations show that in large clusters (such as our birth cluster) three body encounters that produce binaries are extremely rare and the binaries that are produced tend to consist of the most massive stellar components of a cluster (Tohline, 2002). Therefore, if Nemesis exists, it must have formed with the Sun within the Solar Birth Cluster. Since brown dwarfs make of 20-25% of the population of newborn stars (Lada and Lada, 2003), this is not a priori implausible.

However, the work of Davis et al. and Whitmire & Jackson preceded the realization that most stars, including our Sun, were born in clusters. To date, there has been no study examining whether a binary consisting of the Sun and a distant brown dwarf companion would be likely to survive the effects of encounters in the birth cluster. If Nemesis formed with the Sun, then it would also be affected by the close encounters that perturbed our Solar System. But what are the effects of these close encounters on such a star? Given the distance from the our Sun and its low mass, Nemesis would seem to be a easy target, particularly if we hypothesize that there were encounters close enough to sculpt the outer Kuiper Belt and produce Sedna.

Currently, there is no research or data on the effects that a close encounter with other stars in the birth cluster would have on such an object. Likewise, there is no research or data on the effects of a close encounter and its relation to an abrupt Kuiper Belt edge. In this work, we conduct a series of simulations to address all of these problems. We start with the assumption that Nemesis has formed with the Sun and run a scattering simulation. In chapter 2, we will look at the scattering simulation which determines the probability of an event happening (for example Nemesis becoming unbound or KBOs being scattered into Sedna-like orbits). In chapter 3 we will look at the end results from the simulations and discuss what information we can extract from the data, while in Chapter 4 we make our conclusions.

2 Methods

To determine the effects that a close encounter would have on the Solar System, I have created an N-body computer simulation. This simulation begins with a model of the Solar System and then simulates the gravitational effects of a star on the Solar System as it approaches from a large distance, passes, and recedes. This simulation is run multiple times under different conditions, and the combined outcomes of these runs are then used to determine the probability that an event will occur. Possible events include Nemesis becoming unbound from the Sun/Nemesis system, a KBO coming unbound, a KBO being excited to an eccentricity > 0.9, and a Jovian planet being excited to an eccentricity > 0.1. In Section 2.1 I give an overview of my simulation and what we seek to accomplish using it. In Section 2.2, I describe the simulation setup. In Section 2.3 I present the simulation engine and finally in Section 2.4 I talk about how the simulations handles each run and stores the raw data.

2.1 Overview

We start with the idea of the probability of an event occurring ($p_{m,v,b,\theta,\phi}$) at a given value of these variables: mass of incoming star (m), the velocity of the incoming star (v), the impact parameter of the incoming star (b, distance of closest approach in absence of gravity), the inclination angle (θ, measured between line of closest approach and line perpendicular to the ecliptic), and the azimuth angle (ϕ, measured between the projection of the incoming star onto the ecliptic and the initial line between the Sun and Nemesis). From $p_{m,v,b,\theta,\phi}$ we can determine the average cross section

times velocity of an event ($\langle\sigma v\rangle_{event}$) by integrating $p_{m,v,b,\theta,\phi}$ over all possible values:

$$\langle\sigma v\rangle_{event} = \int_{-\infty}^{\infty} dv \frac{1}{\sigma_v^3}\sqrt{\frac{2}{\pi}} v^3 e^{\frac{-v^2}{2\sigma_v^2}} \int_0^{m_{max}} dm \frac{dN}{dm} \int_0^{b_{max}} db\ 2\pi b \int_0^{\pi} d\theta \sin\theta \int_0^{2\pi} d\phi\ p_{m,v,b,\theta,\phi}. \quad (2.1)$$

Here $\frac{dN}{dm}$ is the probability that a random star will have mass between m and m + dm (the IMF), σ_v is the standard deviation of the velocity distribution, m_{max} is determined by the IMF and b_{max} will be discussed in Section 2.2. This expression assumes that the stellar velocity distribution is Maxwellian.

To evaluate $\langle\sigma v\rangle_{event}$, we will utilize the computer simulation to do the integration of four variables, leaving us with just one variable, velocity, for which we can safely account by assuming the distribution of encounter velocities is Maxwellian. The simulation will begin with a model of the Solar System with the Sun, Nemesis, the four Jovian planets and a number of KBOs (see Section 2.2). It will then simulate a close encounter by starting with one or two incoming stars far away with a randomly chosen m, b, θ and ϕ, with each variable weighted differently (see Section 2.2). Once the simulation begins, we compute the paths of all bodies using a Bulirsch-Stoer method (see Section 2.3). When the incoming star has passed the Sun and is very far away, the simulation is stopped and final orbits are calculated for all objects in the Solar System. Then each event in question is analyzed, and we calculate $p_{m,v,b,\theta,\phi}$. With $p_{m,v,b,\theta,\phi}$ know for each event, we can then determine that average cross section of a event happening at a given velocity ($\langle\sigma\rangle$) by integrating over m, b, ϕ and ψ

$$\langle\sigma\rangle = \int_0^{m_{max}} dm \frac{dN}{dm} \int_0^{b_{max}} db 2\pi b \int_0^{\pi} d\theta \sin\theta \int_0^{2\pi} d\phi\ p_{m,v,b,\theta,\phi}. \quad (2.2)$$

As the number of runs becomes to large, the four randomly chosen variables cover the full range of values of each variable (See section 2.4). We then assume that the stellar velocity distribution within the birth cluster follows a Maxwell-Boltzmann distribution. We can therefore integrate $\langle\sigma\rangle$ over all velocities to obtain average cross section time velocity,

$$\langle\sigma v\rangle_{event} = \frac{1}{\sigma_v^3}\sqrt{\frac{2}{\pi}} \int_{-\infty}^{\infty} \langle\sigma\rangle v^3 e^{\frac{-v^2}{2\sigma_v^2}} dv. \quad (2.3)$$

Once $\langle\sigma v\rangle$ is determined, we can obtain the rate at which an event is encountered by multiplying

$\langle \sigma v \rangle$ by the number density in the birth cluster (n_c)

$$\Gamma_{event} = n_c \langle \sigma v \rangle_{event}. \tag{2.4}$$

Given Γ_{event}, we can determine the expected number of occurrences of the event, Λ_{event}, by multiplying Γ_{event} by the total time the Sun is exposed within the cluster. This time will be roughly the time for which the cluster survives before mass evaporation leads it to disperse, t_{life}. Since t_{life} is estimated to be between one and four crossing times (see Section 1), we will take t_{life} $\sim t_{cross}$. If the true lifetime is longer then an event's probability will be increased proportionately. Thus, we have

$$\Lambda_{event} = \Gamma_{event} t_{cross}. \tag{2.5}$$

To compute the overall probability that an event will happen (P_{event}), we assume the events follow a Poisson distribution. For a Poisson process with expectation value Λ, the probability of k occurrences is

$$P(k) = \frac{\Lambda^k e^{-\Lambda}}{k!}. \tag{2.6}$$

We want to compute the probability that an event will occur at least once. To calculate this, we subtract the probability an event will not occur (k = 0) from unity

$$P_{event} = 1 - P(0). \tag{2.7}$$

This then leads us to

$$P_{event} = 1 - e^{-\Lambda}. \tag{2.8}$$

The initial conditions of the birth cluster are unknown to us, so we cannot directly compute Γ_{event} and t_{cross}. However, we can estimate them in terms of the cluster surface density (Σ_c) and cluster mass (M_c). Γ_{event} depends on the number density of stars within the cluster, n_c, and the velocity dispersion, σ_v. The number density is implicitly given by:

$$M_c = \frac{M_\odot}{5} n_c \frac{4}{3} \pi r_c^3 \tag{2.9}$$

where r_c is the radius of the cluster and we use $\frac{M_\odot}{5}$ as the average mass per star (Chabrier, 2005). The cluster surface density is given by

$$\Sigma_c = \frac{M_c}{\pi r_c^2}. \tag{2.10}$$

The crossing time is

$$t_{cross} = \frac{r_c}{\sigma_v}. \tag{2.11}$$

Solving these equations, we obtain

$$n_c = \frac{15\pi^{\frac{1}{2}}\Sigma_c^{\frac{3}{2}}}{4M_\odot M_c^{\frac{1}{2}}} \tag{2.12}$$

$$t_{cross} = \frac{M_c^{\frac{1}{4}}}{G^{\frac{1}{2}}(\pi\Sigma_c)^{\frac{3}{4}}} \tag{2.13}$$

$$\sigma_v = G^{\frac{1}{2}}\left(\pi\sigma M_c\right)^{\frac{1}{4}}. \tag{2.14}$$

Given these relations, we can estimate Λ_{event} and P_{event} in terms of M_c and Σ_c.

2.2 Setup

In each simulation we put the Sun, a particle of mass $M_\odot$, at the origin. Nemesis's mass (M_N) was set to one of three values: 0, $0.02M_\odot$ or $0.08M_\odot$. We did this because Nemesis' mass is unknown and could in theory be any size below $0.08M_\odot$, the hydrogen burning limit (see Section 1). Including different possible masses for Nemesis enables us to determine whether the probability of an event occurring depends on Nemesis's mass. This could allows us to identify possible mass constraints on Nemesis. In our setup, Nemesis always begins at its aphelion with a semi-major axis (a_N) of 1000 AU. Given this, its starting distance from the Sun is given by $r_o = \frac{a_N(M_\odot+M_N)}{M_\odot}$, and we place it on the x-axis. We then randomly select an eccentricity (e_N) between 0.0 and 0.4 and calculate Nemesis's starting orbital velocity

$$v_o = \sqrt{G(M_\odot + M_N)\frac{1-e_N}{a_N}} \tag{2.15}$$

as if it were orbiting clockwise in the xy plane around the Sun (i.e. the starting velocity has only a negative y component). Finally, the program randomly selects an angle from zero to 2π and

then rotates Nemesis's xy-position and xy-velocities by the selected angle to ensure that Nemesis is randomly oriented relative to the incoming star(s).

We then place the planets in the simulation. We only include the four Jovian planets (Jupiter, Saturn, Uranus and Neptune) not the Terrestrial planets (Mercury, Venus, Earth and Mars) or the astroid belt. We excluded these objects because the perturbation from either the incoming star(s) or Nemesis would completely disrupt the orbits of the Jovian planets well before disturbing the orbits of the other objects, and thus including them would consume CPU time while providing little insight. The masses of the four Jovian planets (as well all KBO objects) were set to zero. This is done because we are looking to determine the effects of the perturbations of Nemesis and the incoming star(s) and not the perturbations from interaction between objects within the solar system. Also, given that these objects have such a small mass relative to the Sun and the incoming star(s), their gravitational effects will be negligible. We determine the orbits of each Jovian in the same way that Nemesis's orbit, with the semi-major axis and eccentricity taken from Carroll and Ostlie (2007). These values can be found in Table 2.1. We also rotate each Jovian's orbit by a random angle from zero to 2π to randomize the phase.

Table 2.1: Jovian Orbit Properties. Data obtained from Carroll and Ostlie (2007)

Planet	Semi-Major Axis (AU)	Eccentricity
Jupiter	5.2044	0.0489
Saturn	9.5826	0.0565
Uranus	19.2012	0.0457
Neptune	30.0476	0.0113

In order to recreate the initial conditions of the Solar System, we set up the Kuiper Belt to correspond to the theorized initial surface density and gradual decline. We place a total of 320 KBOs in the simulation arranged in 32 concentric circles with ten KBOs per ring. Within each ring, all ten KBOs are evenly spaced, creating an angle of $\frac{\pi}{5}$ between each KBO. The first ring has a radius of 35 AU, and each successive ring's radius is 15 AU larger, leaving the last ring at 500 AU. Thus, the KBOs are arranged like a wheel with ten spokes radiating outward, with the Sun at

the center in the xy-plane. We make the KBOs massless (as mentioned above) and give them zero eccentricity. This setup is intended to allow easy examination of perturbation effects from both the incoming star(s) and Nemesis after the simulation was finished running. We determine the starting velocities for the KBOs using the same equation (equation 2.15) used for Nemesis and the Jovians.

Next we set up the incoming star(s). The first step is to determine the mass of one incoming star by randomly choosing from the initial mass function (IMF). The probability that the incoming star has a mass from m to $m + dm$ is giving by $p(m) = K\xi(m)$ where K is a normalization factor and

$$\xi(m) = \begin{cases} (\frac{m}{m_1})^{-\alpha_0} & : m_l < m \leq m_1 \\ (\frac{m}{m_1})^{-\alpha_1} & : m_1 \leq m \leq m_2 \\ (\frac{m}{m_1})^{-\alpha_1}(\frac{m}{m_2})^{-\alpha_2} & : m_2 < m \leq m_u \end{cases} \tag{2.16}$$

with the following values determined through observational means reported by Kroupa (2002)

$$\begin{aligned} \alpha_0 &= +0.3 \quad : 0.01 < \tfrac{m}{M_\odot} \leq 0.08 \\ \alpha_1 &= +1.3 \quad : 0.08 < \tfrac{m}{M_\odot} \leq 0.50 \\ \alpha_2 &= +2.3 \quad : 0.50 < \tfrac{m}{M_\odot} \leq 120 \end{aligned} \tag{2.17}$$

We then determine whether the incoming star is alone or part of a binary system. We set the probability that the incoming star is in a binary based on a rough fit to the binary mass function versus primary mass reported by Lada (2006) and Kouwenhoven et al. (2007) for low and high mass stars, respectively. The binary fraction we adopt is

$$f_{binary} = \begin{cases} 0.2 & : m < 0.5\ M_\odot \\ 0.2 + 0.8\left(\frac{m-0.5}{1.5}\right) & : 0.5\ M_\odot \leq m \leq 2.0\ M_\odot \\ 1.0 & : m > 2.0\ M_\odot \end{cases} \tag{2.18}$$

We randomly determine whether the primary is a binary, and, if so we select a secondary from the IMF. We took the first star to be the primary star, so if the mass selected for the second star is greater than the first, that mass is rejected and another is selected.

Next we choose the impact parameter b, the closest approach the incoming star would have with the Sun in the absence of gravity. The cross-sectional area available at impact parameter

b, and thus the probability that an incoming star has an impact parameter between b and db, is proportional to b. We therefore select a value from 0 to b_{max}, with the probability proportional to b. We take b_{max} to be 2000 AU because we found that encouters with larger b essentially never perturbed any part of the solar system significantly.

We then placed the incoming star(s) onto our coordinate system. In the case of just one incoming star, we placed the star with x-coordinate 10,000 AU, y-coordinate of zero and z-coordinate of b. The star was given its initial velocity as described in Section 2.4 just in the negative x direction, with a velocity of zero in both the y and z directions. When a binary system was identified for the close encounter, the center of mass of the binary system was placed in the same coordinates as for a single star. We then selected the orbital properties of the binary system. Based on observations, we adopt a period (τ) distubution

$$p(\log \tau) = \frac{1}{\sqrt{2\pi\sigma^2_{\log \tau}}} e^{\frac{-(\log \tau - \overline{\log \tau})^2}{2\sigma^2_{\log \tau}}} \tag{2.19}$$

where $\overline{log\tau} = 4.8$, $\sigma_{log\tau} = 2.3$ and τ is in days (Duquennoy and Mayor, 1991). Given τ, the semi-major axis is then

$$a = \sqrt[3]{\frac{G\tau^2(m_1 + m_2)}{4\pi^2}}. \tag{2.20}$$

Next we randomly select an eccentricity from a uniform distribution going from 0.2 to 0.8 (Duquennoy and Mayor, 1991). With the eccentricity and semi-major axis we then determined orbital dynamics of the binary system using same equations used with Nemesis and the Jovians. We place both stars along the line y=0, z=b. The displacement of the two stars from the center of mass is

$$r_1 = \frac{a(m_1 + m_2)}{m_1} \tag{2.21}$$

$$r_2 = \frac{a(m_1 + m_2)}{m_2}. \tag{2.22}$$

Thus the x-component of the primary star was 10,000AU - r_1 and the secondary star was 10,000AU + r_2. The velocities were obtained using the same formula as Nemesis. We then added the velocity

of the center of mass to create an orbiting binary system with its center of mass moving towards the Sun at the initial velocity.

The set up as described placed both the Solar ecliptic and the plane of orbit for the binary stars parallel to one another. However, these two planes should completely randomly oriented relative to each other. To do this, we select three random angles (θ, ϕ and ψ) between zero and 2π. θ is used to transform their positions and velocities of both stars about the center of mass clockwise in the xy-plane. ϕ then transforms the two stars by rotating then about the line that was parallel with the the x-axis and passes through their center of mass. Finally, ψ transforms them about the line parallel with the y-axis and through their center of mass.

The final step before starting the run is to orient the Solar ecliptic. The set up at this point places the incoming system edge-on relative to the ecliptic, but we would expect the incoming system to be at any angle relative to the ecliptic with equal probability. Since we already rotated the each of the Jovians and Nemesis in the xy-plane, we only have to consider rotating the Solar System about the x-axis and the y-axis. We randomly select two more angles (α and β) between zero and 2π. Using α as the angle the ecliptic was rotated about the x-axis and β the angle the ecliptic was rotated about the y-axis, we transform the positions and velocities of of each planet, KBO and Nemesis by

$$\begin{aligned}
X_{new} &= X_{old}\cos\beta + Y_{old}\sin\beta\sin\alpha \\
Y_{new} &= X_{old}\cos\alpha + Y_{old}\sin\alpha \\
Z_{new} &= X_{old}\sin\beta + Y_{old}\cos\beta\sin\alpha \\
V_{x-new} &= V_{x-old}\cos\beta + V_{y-old}\sin\beta\sin\alpha \\
V_{y-new} &= V_{x-old}\cos\alpha + V_{y-old}\sin\alpha \\
V_{z-new} &= V_{x-old}\cos\beta + V_{y-old}\cos\beta\sin\alpha
\end{aligned} \tag{2.23}$$

2.3 Engine

The equations of gravity which the engine solves are given by

$$\ddot{x_i} = \sum_{j=1, j\neq i}^{N} \frac{GM_j}{r_{ij}^2} \frac{x_j - x_i}{|\vec{r_{ij}}|} \tag{2.24}$$

$$\ddot{y_i} = \sum_{j=1, j\neq i}^{N} \frac{GM_j}{r_{ij}^2} \frac{y_j - y_i}{|\vec{r_{ij}}|} \tag{2.25}$$

$$\ddot{z_i} = \sum_{j=1, j\neq i}^{N} \frac{GM_j}{r_{ij}^2} \frac{z_j - z_i}{|\vec{r_{ij}}|} \tag{2.26}$$

where $\vec{r_{ij}}$ is the vector going from object i to object j and N is the total number of objects within the simulation. We solve these equations using an engine that is based on the Bulirsch-Stoer method (Press et al., 1988). The Bulirsch-Stoer Method is a very effective numerical method for solving smooth ODEs. The Bulirsch-Stoer method relies of these techniques: Richardson extrapolation, the use of rational functions as fitting functions for the Richardson extrapolation and the modified midpoint method.

Richardson extrapolation considers the final result of a numerical calculation as itself being an analytic function of an adjustable parameter of the step size h. By varying the value of h, the Richardson extrapolation method can construct an approzimate analytic function for the result of the calculation as a function of h, and evaluate in the limit $h \to 0$. The next concept is to have the Richardson extrapolation construct the analytic function approximation as a rational function. Rational functions have the advantage over polynomial functions that they lack singular points in the complex plane. If a polynomial function is used in Richardson extrapolation, the size of h is limited by the radius of convergence dictated by the singular point. Rational functions do not have this limitation and thus can use very large h with minimal error. Lastly, the Bulirsch-Stoer Method uses the modified midpoint method to advance the rational function obtained by the Richardson extrapolation by a step size of H by breaking it down into n smaller step sizes of h where $h = \frac{H}{n}$. The numerical values of the smaller step sizes are then evaluated to the average of the surrounding steps, advancing the function bit by bit until the full step size of H is completed (Press et al., 1988).

2.4 Runs and Data

Each run begins with the incoming star(s) at a distance of 10,000AU from the Sun, and ends when the star(s) returns to that distance. We record the initial and final positions and velocities for all objects within the simulation, plus all randomly selected variables. From the final velocities, we then compute the eccentricities of all objects orbiting the Sun. We consider three possible masses for Nemesis (0.0, 0.02 and $0.08 M_{\odot}$) and forty possible initial velocities for the incoming star(s), ranging from 0.5km/s to 20.0km/s in 0.5km/s intervals. We preform a simulation at each of the three possible Nemisis masses beginning with the lowest incoming star velocity, with all randomly determined quantities (incoming star mass, impact parameter, angle, etc.) held fixed. We then repeat this procedure, incrementing the incoming star velocity each time. This gives us 120 total runs per file, and we complete 1644 such sets of 120 runs. We will call data from these runs alone Type I. Also, to examine the effect of lower velocity encounters in more detail, we ran another set of simulations in which the incoming star velocity starts at 0.1km/s and increased the velocity per run by 0.1km/s up to 2.5 km/s. This set of simulations was only done for a Nemesis mass of $0.02 M_{\odot}$ and therefore has only 25 runs per file, and we completed 1865 such sets of 25 runs. We will call data from these runs alone Type II.

We use a Monte Carlo integration method to evaluate the integral in equation 2.2. As our four random variables change with each run and the number of runs approaches large numbers, we will have sampled each integrand at the full range of the variables and thus reconstructed the integrals. Given this, equation 2.2 will then be reduced to

$$\langle \sigma \rangle = p(v)_{event} \pi b_{max}^2 \tag{2.27}$$

where $p(v)$ is the number of events occurring at a given velocity divided by the total number of runs at said velocity. Once $\langle \sigma \rangle$ has been constructed for each event in which we are interested, we can then numerically determine $\langle \sigma v \rangle_{event}$ in equation 2.3.

3 Analysis

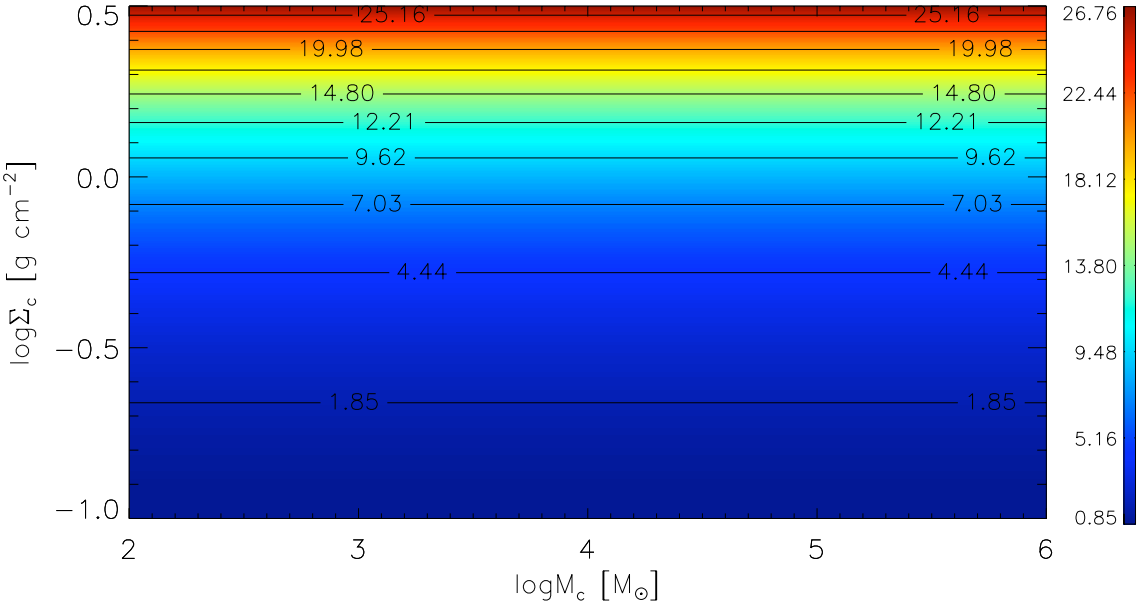

Figure 3.1: Expected number of encounters between the Sun and another star with $b < 2,000$ AU per cluster crossing time, as a function of cluster mass M_c and surface density Σ_C. The number of encounters is independent of M_c. This is because if $\langle\sigma\rangle$ is constant, then the integral in equation 2.3 is proportional to M_c, which leaves $\Lambda \propto \frac{n_c t_{cross}}{\sigma_v^3} M_c \propto M^0$.

The simulation of our Solar System was started with 320 KBOs, four Jovian planets and one brown dwarf star (See Section 2.2). After the simulation stopped, the eccentricities of all objects were determined, and the effects of the close encounter could be seen. In this section we will look at

the effects of close encounters. To set the stage, we first compute the expected number of encounters the Sun experiences with $b < 2,000$ AU per cluster crossing time. We do so by making $p(v) = 1$ for all velocities in equation 2.27, and thus $\langle\sigma\rangle = \pi b_{max}^2$ where $b_{max} = 2000$ AU. We can then calculate Λ from equations 2.3, 2.4 and 2.5. We show the results in Fig. 3.1. In this and all similar figures, we consider clusters with mass $M_c = 10^2 - 10^6\ M_\odot$, and surface density $\Sigma_c = 10^{-1} - 10^{0.5}\ gcm^{-2}$. As we can see in Fig. 3.1, the number of expected encounters ranges from ~ 1 at low surface densities up to ~ 20 at the other extreme. With this background, in Section 3.1 we discuss how close encounters affect the four Jovian planets, and whether the effects depends on Nemesis's mass. In Section 3.2 we look at the effects on the KBOs. Lastly in Section 3.3, we will examine the effects of a close encounter on Nemesis itself and we compute the likelihood of Nemesis becoming unbound.

3.1 Effects of Close Encounters on the Jovian Planets

Our Solar System as we see it today is well ordered (See Section 1); therefore, any proposed birth cluster properties that would cause one of the Jovian planets to have an eccentricity greater than 0.1 can be rejected. We construct $p(v)_{Jovian>0.1}$ from equation 2.27 by dividing the number of times a given Jovian is excited to an eccentricity above 0.1 at a given velocity by the number of runs at said velocity. Next we multiply $p(v)$ by πb_{max}^2 to obtain $\langle\sigma\rangle_{Jovian>0.1}$, or the average cross sectional area in which a Jovian planet will be excited to an eccentricity greater than 0.1 at a given velocity. First, we investigate our results' dependency on Nemesis's mass. Figure 3.3 shows the $\langle\sigma\rangle_{Jovian>0.1}$ vs. velocity from data Type I for each Jovian. In each plot, three different lines that represent $\langle\sigma\rangle_{Jovian>0.1}$ from simulations with different masses of Nemesis. Using the three data from the three different Nemesis masses, we compute the mean value, $\mu(v)$, and the variance, $s(v)$, of $\langle\sigma\rangle_{Jovian>0.1}$. We then compare each run of fixed Nemesis mass with $\mu(v)$ using a χ^2 test. We report the results in Table 3.1. The data shows no dependence of the results on Nemesis's mass. For the rest of the paper, unless explicitly stated, all calculations will use all data without regard to Nemesis's mass.

Having established this result, we now compute $\langle\sigma\rangle$ and $\Lambda_{Jov>0.1}$ (equation 2.5), for each Jovian. We show the results in Fig. 3.2 and 3.4. Looking at Fig. 3.4, we see that across all reasonable values of M_c and Σ_c, the number of expected encounters in which any of the Jovian planets is excited is much less than one.

We next use $\Lambda_{Jov>0.1}$ in equation 2.8 to compute the probability of a Jovian being excited to an eccentricity greater than 0.1. Figure 3.5 shows the results. Looking at these plots, we see that the probability of exciting a Jovian to an eccentricity greater than 0.1 is very low across all cluster masses and surface densities. For all four Jovians, the only conditions under which the probability goes above 1% are when the cluster is very low mass and very high density. The highest probability we obtain in any of the figures is just above 9%, for Neptune. Close encounters have minimal effects on the Jovian planets. Furthermore, as we increase the birth cluster's mass at fixed Σ_c the probability of exciting a Jovian decreases. This is because $\sigma_v \propto M_c^{\frac{1}{4}}$ (equation 2.14), so σ_v rises with M_c. Looking back to Fig. 3.2, we see that $\langle\sigma\rangle$ is dramatically lower at velocities greater than 3.0 km/s than at lower velocities. At higher velocities, a star has less time to interact with our Solar System and thus its effects on the Solar System are greatly reduced. This, coupled with an encounter rate that is independent of M_c (Fig. 3.1), leads us to the conclusion that well ordered planets can form in birth clusters with membership size greater than 10^4.

To understand why our conclusion is at odds with that of Adams (2010), it is helpful to define a velocity-dependent maximum impact parameter for a given interaction by

$$b(v) = \sqrt{\frac{\langle\sigma\rangle}{\pi}}. \tag{3.1}$$

We show this quantity in Fig. 3.6. We see that at very low velocities (around 0.1 km/s), the impact parameter a very large ($\sim$ 1700 AU for Neptune and $\sim$ 1200 AU for Jupiter, the two extremes). However, as we move to about 0.5 km/s, there is a drastic drop off in $b(v)$, with Neptune falling to $\sim$ 700 AU and Jupiter to $\sim$ 300 AU. Above 3.0 km/s, $b(v)$ is less than 150 AU for Neptune and less than 75 AU for Jupiter, and it continues to decrease (much less drastically) as we move to the higher velocities. This shows that even though at low velocities the impact parameter is big, at

slightly higher velocities $b(v)$ is significantly less than estimated impact parameter of 225 AU used by Adams (2010) to place an upper limit on the birth cluster membership size.

Nemesis Mass	ν	χ^2	$Q(\frac{\nu}{2}, \frac{\chi^2}{2})$
Jupiter			
0 $M_\odot$	16	9.296	0.86
0.02 $M_\odot$	16	10.22	0.81
0.08 $M_\odot$	16	10.98	0.75
Saturn			
0 $M_\odot$	21	16.16	0.71
0.02 $M_\odot$	21	15.24	0.76
0.08 $M_\odot$	21	16.00	0.72
Uranus			
0 $M_\odot$	25	17.88	0.81
0.02 $M_\odot$	25	11.73	0.98
0.08 $M_\odot$	25	18.67	0.77
Neptune			
0 $M_\odot$	32	20.37	0.92
0.02 $M_\odot$	32	11.48	0.99
0.08 $M_\odot$	32	24.15	0.80
Nemesis			
0 $M_\odot$	39	20.93	0.98
0.02 $M_\odot$	39	21.80	0.98
0.08 $M_\odot$	39	27.27	0.90

Table 3.1: Results of a χ^2 comparison between $\langle\sigma\rangle$ for each Nemesis mass, and the mean of $\langle\sigma\rangle$ over all three different Nemesis mass. We report results for $\langle\sigma\rangle$ for five events: Jupiter achieving $\epsilon > 0.1$, Saturn achieving $\epsilon > 0.1$, Uranus achieving $\epsilon > 0.1$, Neptune achieving $\epsilon > 0.1$ and Nemesis itself becoming unbound. The degrees of freedom for the test, ν, is the number of velocity bins with useable data (i.e. if the a given velocity bin is empty for all three masses, then that bin is not counted as a degree of freedom). $Q(\frac{\nu}{2}, \frac{\chi^2}{2}) = 1 - P(\frac{\nu}{2}, \frac{\chi^2}{2})$ where $P(a, x)$ is the incomplete gamma function, is the chi-square probability function which ranges from 0 to 1 where 0 is low confidence that the data were drawn from the same parent distribution and 1 is high confidence (Press et al., 1988). Note that all $Q(\frac{\nu}{2}, \frac{\chi^2}{2})$ values are close to unity, indicating good agreement between the data sets.

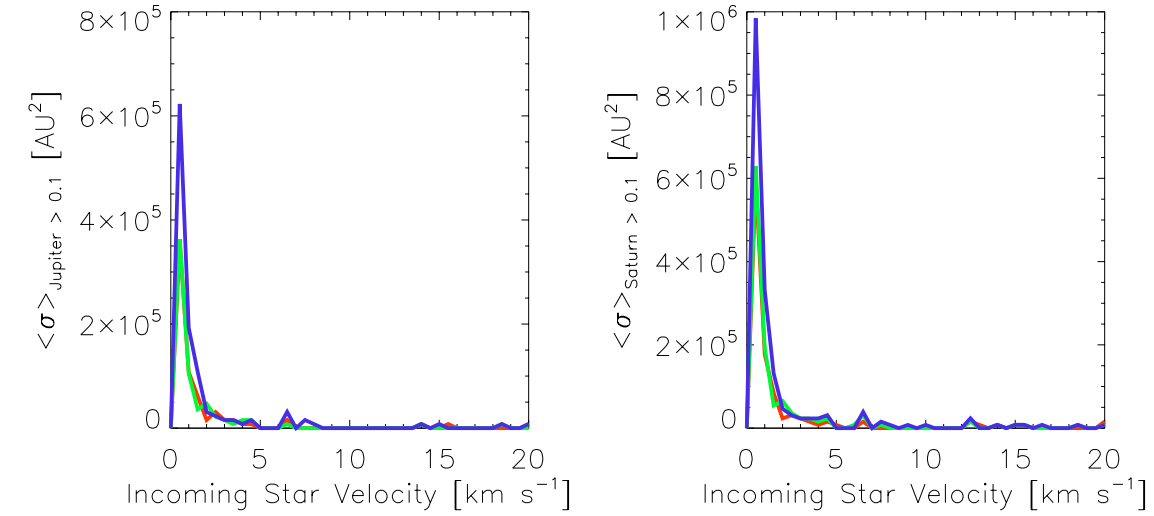

(a) Jupiter

(b) Saturn

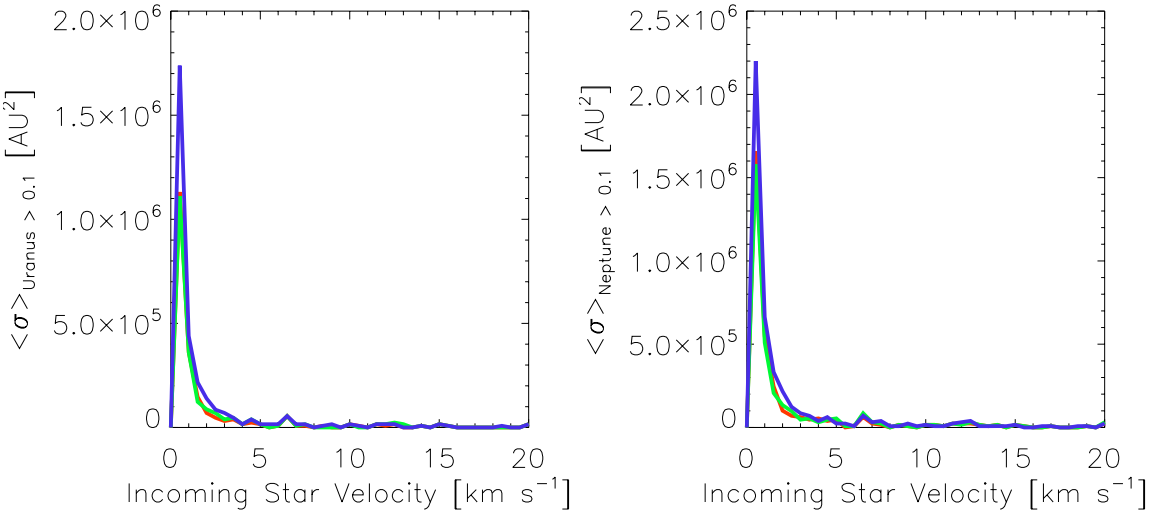

(c) Uranus

(d) Neptune

Figure 3.2: $\langle\sigma\rangle_{Jovian>0.1}$ vs. velocity for each Jovian. In each graph, the red line is for a simulation with Nemesis mass of 0 $M_{\odot}$, green line is when Nemesis mass is 0.02 $M_{\odot}$ and the blue line is when Nemesis mass is 0.08 $M_{\odot}$. $p(v)$ in these graphs is determined only by data Type I only (See Section 2.4).

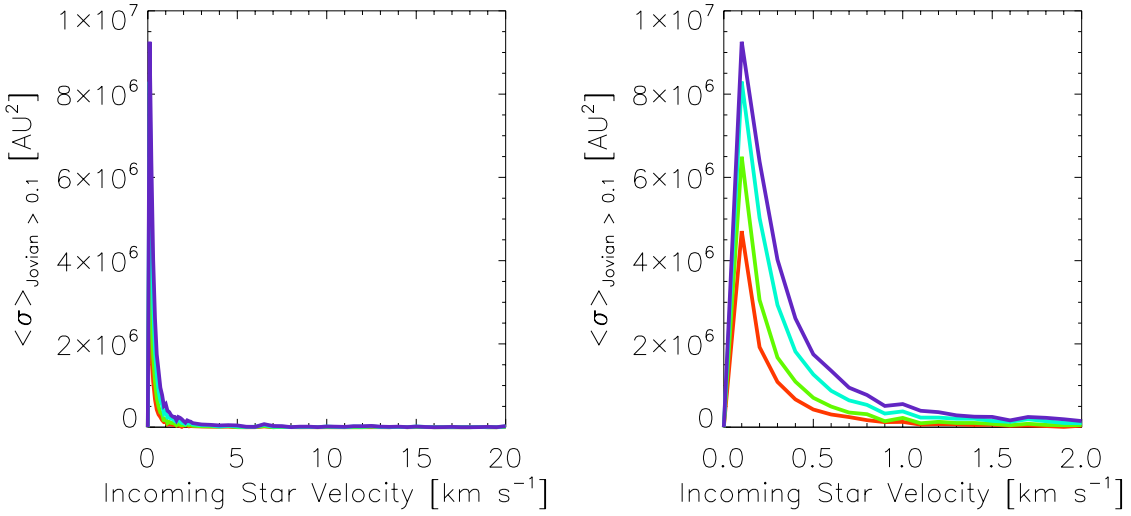

(a) 0 $km/s \leq v \leq$ 20.0 km/s

(b) 0 $km/s \leq v \leq$ 2.0 km/s

Figure 3.3: $\langle\sigma\rangle$ for all for Jovian planets using both Type I and Type II data. Jupiter is the red line, Saturn is the green line, Uranus is the blue line and Neptune is the purple line. Panel (a) the velocity ranges from 0 to 20.0 km/s while in panel (b) the velocity ranges from 0 to 2.0 km/s.

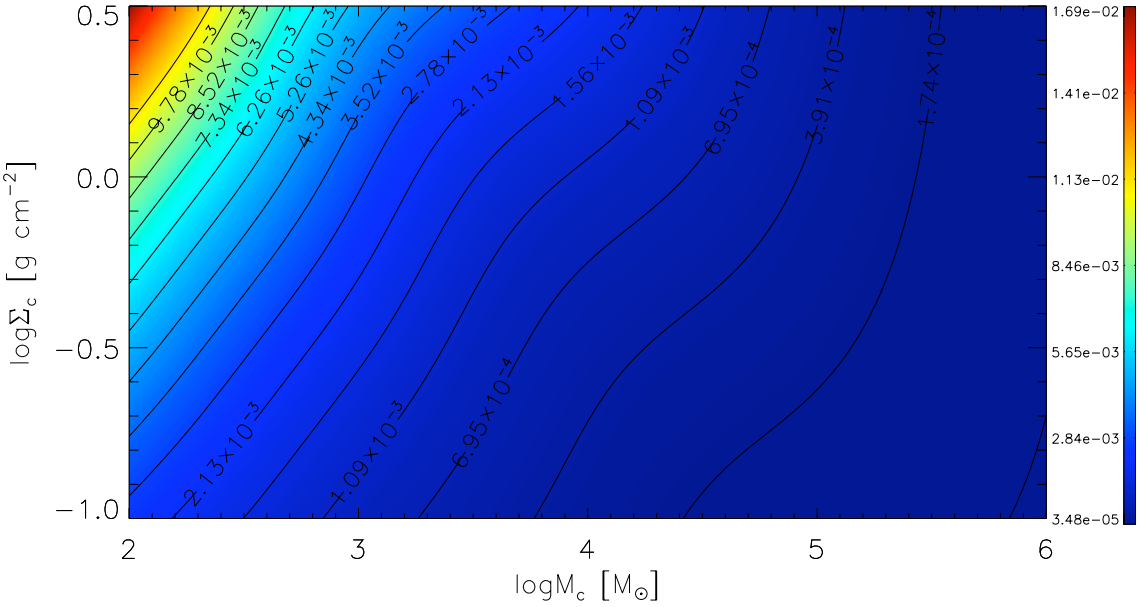

(a) Jupiter

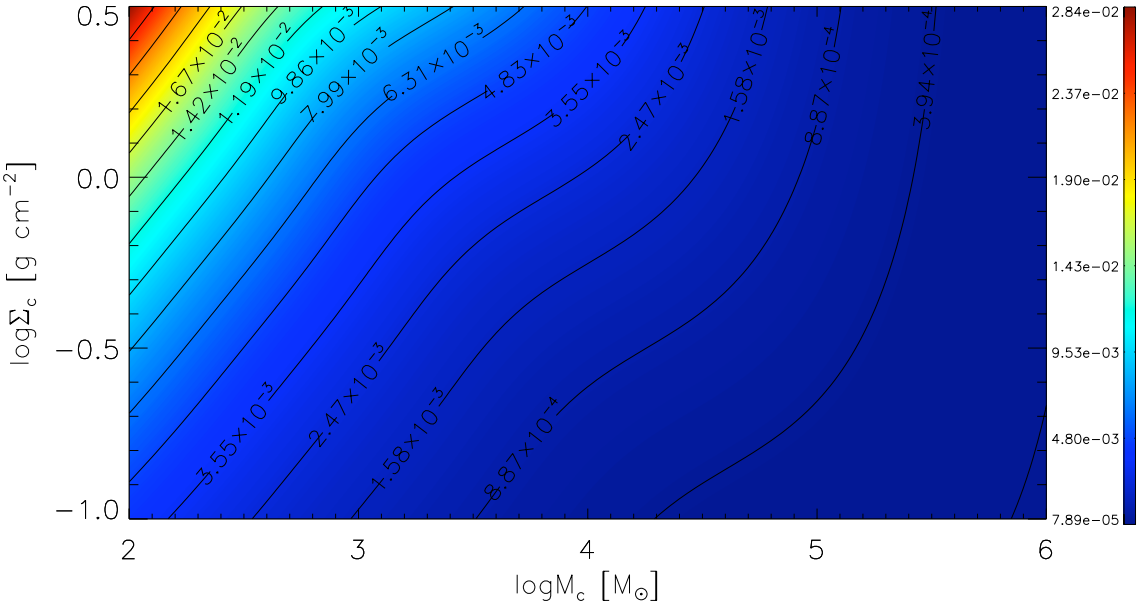

(b) Saturn

Figure 3.4

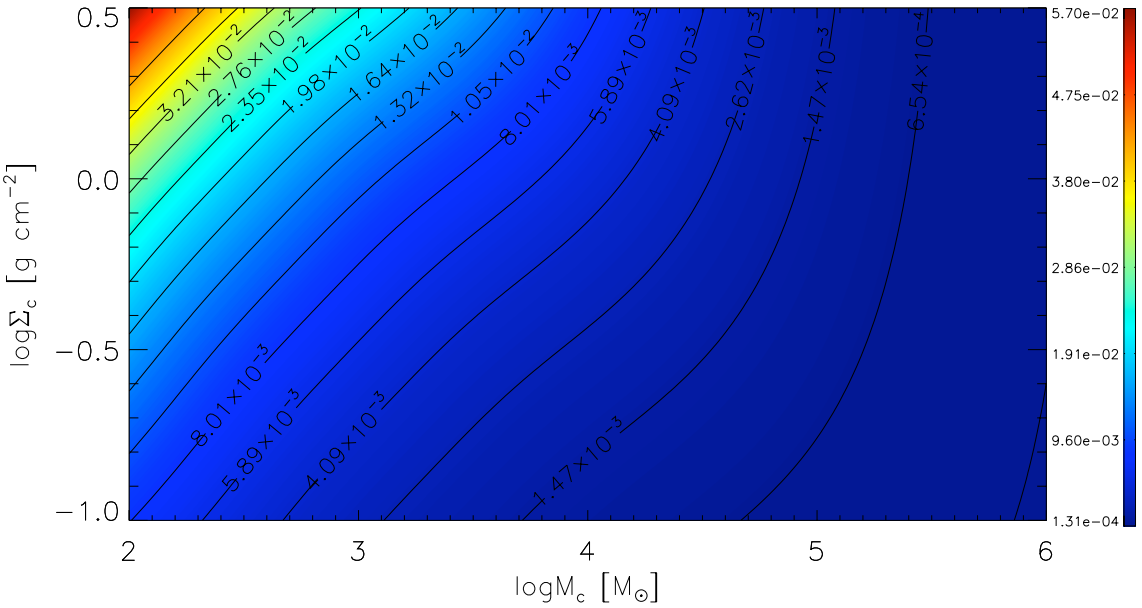

(c) Uranus

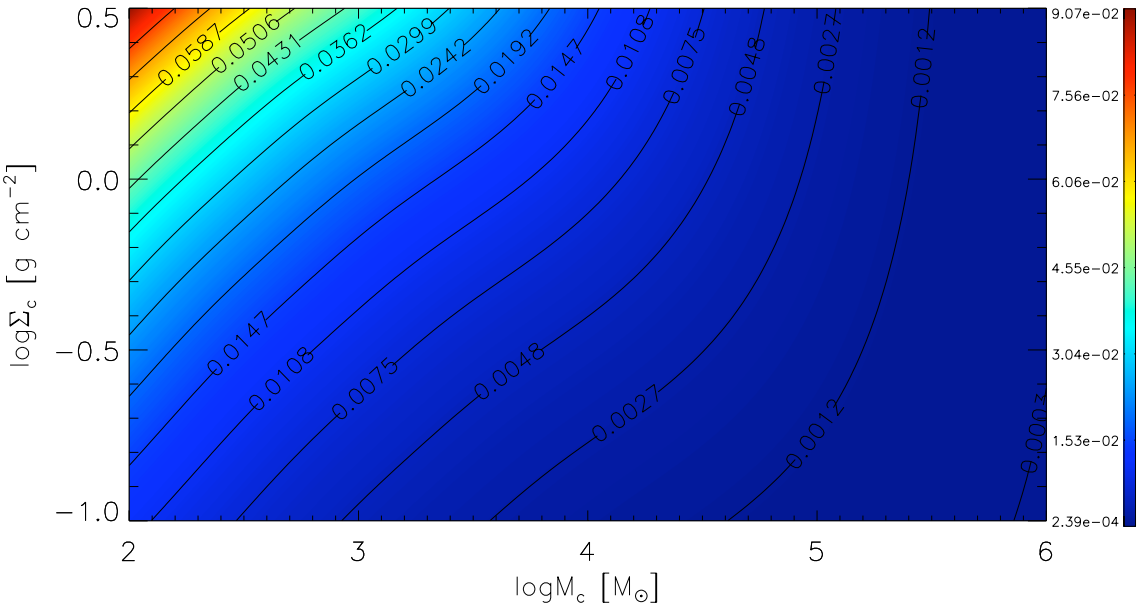

(d) Neptune

Figure 3.4: Expected number of encounters per crossing time that will result in a Jovian planet's eccentricity being excited to greater than 0.1, as a function of $\log M_c$ and $\log \Sigma_c$. As we can see, the expected number of encounters is $\ll 1$ for all Jovian planets at all values of M_c and Σ_c.

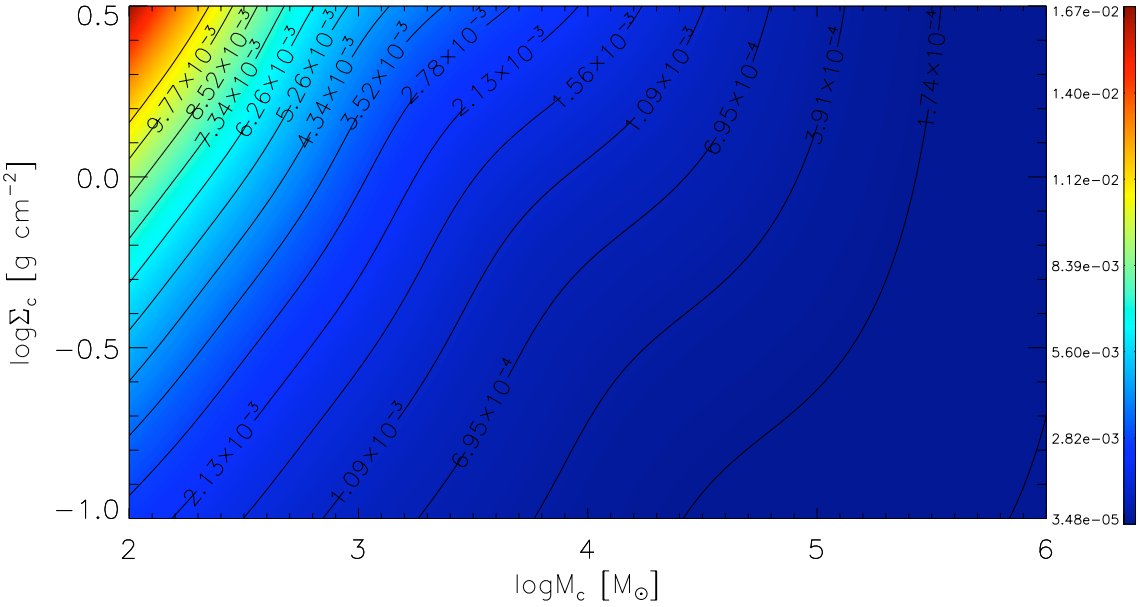

(a) Jupiter

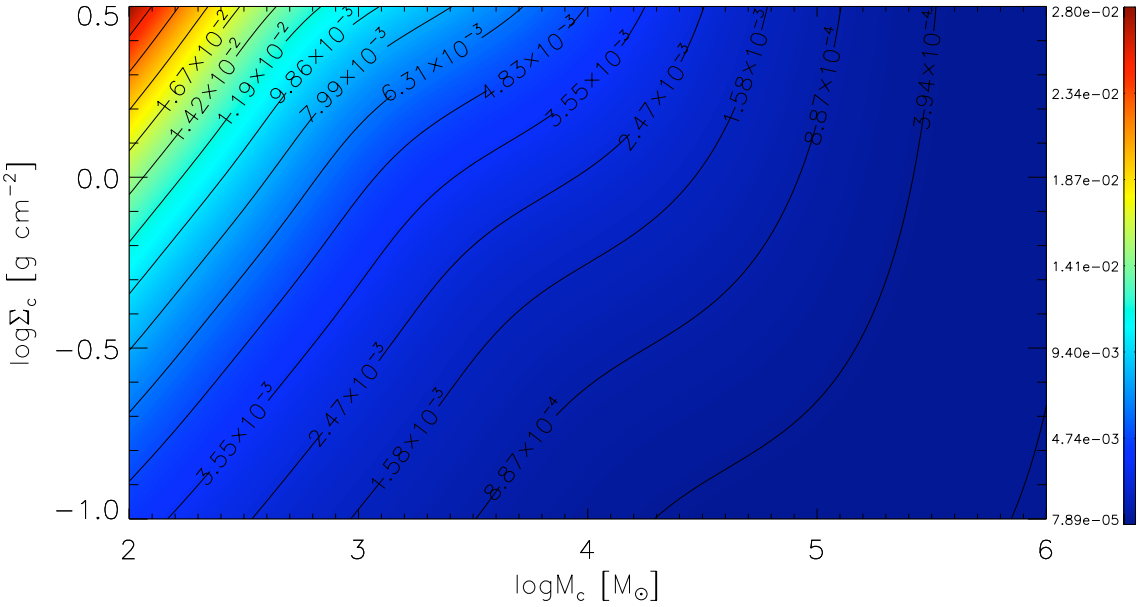

(b) Saturn

Figure 3.5

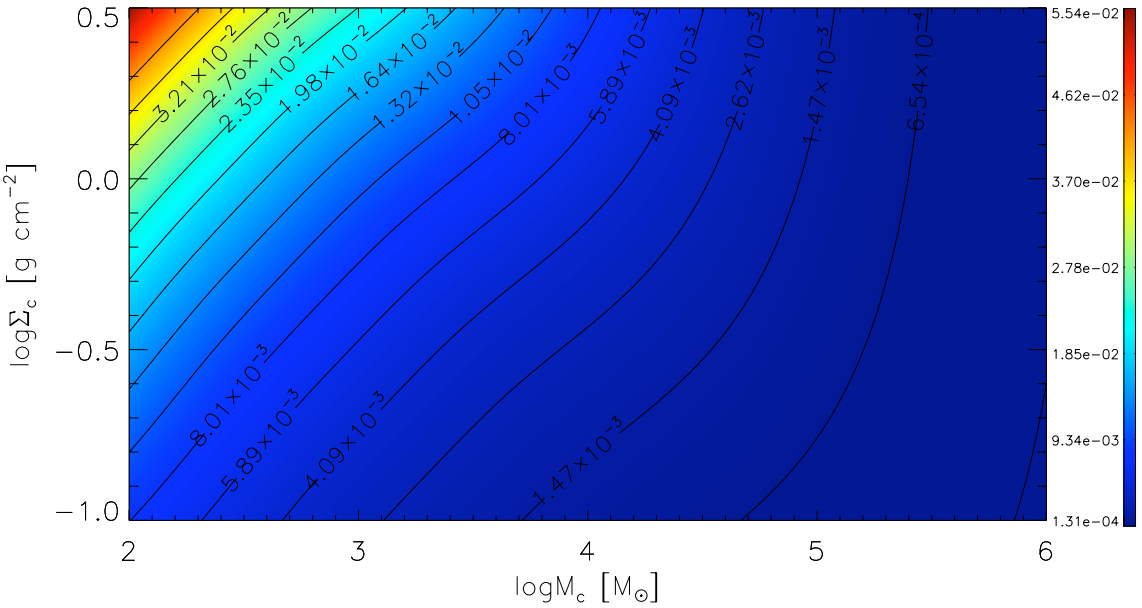

(c) Uranus

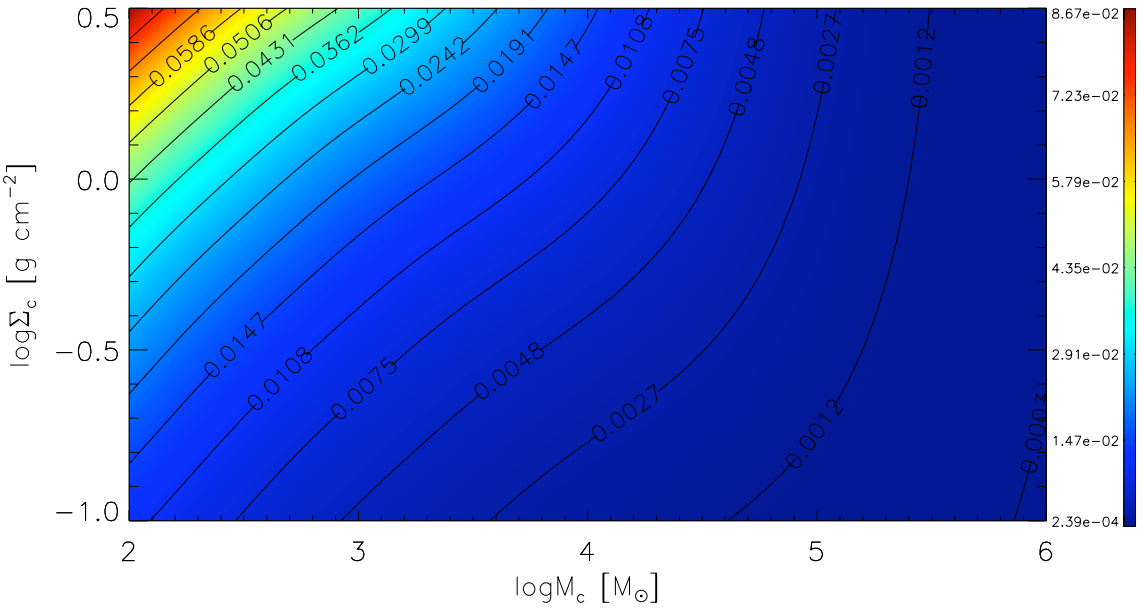

(d) Neptune

Figure 3.5: Probability that, in one crossing time, a Jovian will be excited to an eccentricity greater than 0.1, as a function of $\log M_c$ and $\log \Sigma_c$. The probability of exciting a Jovian is very low across the board, especially in a high mass cluster.

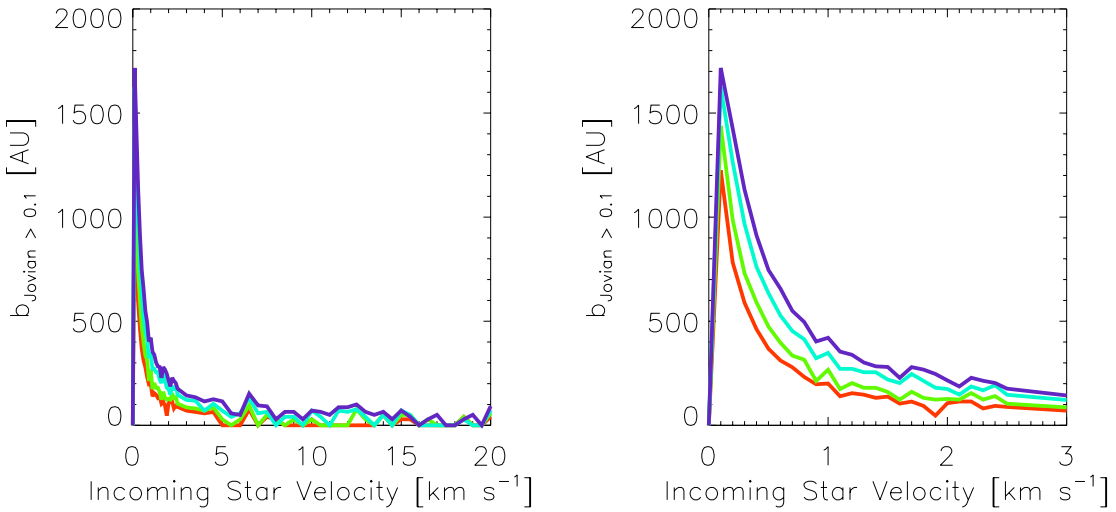

(a) 0 $km/s \leq v \leq 20.0$ km/s

(b) 0 $km/s \leq v \leq 3.0$ km/s

Figure 3.6: Effective impact parameter, b (see equation 3.1) for exciting a Jovian to eccentricity greater than 0.1 vs. velocity of incoming star. Jupiter is the red line, Saturn is the green line, Uranus is the blue line and Neptune is the purple line. At very low velocities, b is large. However, at this low velocity, a small increase in velocity produces a dramatic decreases in b.

3.2 Effects of Close Encounters on the Kuiper Belt

3.2.1 Exciting KBO orbits

The Kuiper Belt is home to Sedna, an object which is irregular for its kind (see Section 1). We would like to know what is the probability that a close encounter was responsible for producing a Sedna-like object. To do this, we first constructed $p(v, n, d)$, where n is the number of KBOs excited to an eccentricity between 0.5 and 1.0 in distance bin d (for our simulation, n goes from 0 to 40). $p(v, n, d)$ is constructed by taking the number of times n KBOs has an eccentricity greater than 0.5 but less than 1.0 from distance bin d at velocity v and dividing by the product of the total number of runs at velocity v and forty (the number of KBO's in each bin). From this we obtained $\langle\sigma(v, n, d)\rangle$ from equation 2.27 and then $\langle\sigma v\rangle_{nd}$ from equation 2.3. We then calculated the total average cross section times velocity at distance bin d by summing all the average cross sections times velocity for a given n,

$$\langle\sigma v\rangle_d = \sum_{n=1}^{40} n\langle\sigma v\rangle_{nd}. \tag{3.2}$$

From this, we were then able to calculate Λ_d from equations 2.4 and 2.5. With Λ_d, we then calculated the probability of exciting at least x KBOs in a given distance bin by summing all of the $P(k)$ for $k = x$ to $k = 40$, i.e.

$$P_d = \sum_{k=x}^{40} \frac{\Lambda_d^k e^{-\Lambda_d}}{k!}. \tag{3.3}$$

Figure 3.7 shows us the probability of exciting just one KBO to an eccentricity between 0.5 and 1.0 in the distance range of 35 AU to 80 AU and 455 AU to 500 AU. The probability of exciting a KBO into a Sedna-like object in the 35 AU to 80 AU range is low ($\sim$13%) for very low mass, high Σ clusters, and the probability falls off as mass is increased, falling below 2% at about $10^4 M_\odot$. The outer bin is more likely to produce a Sedna-like object. At the very low mass, high Σ extreme, the probability is $\sim$80%, but as we increase the cluster's mass we see that the probability falls below 14% at $10^4 M_\odot$ and continues to drop.

3.2.2 Stripping off KBOs

The Kuiper Belt shows a drastic drop in object density at about 50 AU, which is counter to current understanding of solar nebula formation (see Section 1). Disk truncation by a close encounter has been hypothesized as a candidate explanation for this phenomenon. To investigate the validity of this hypothesis we create a $p(v, n, d)$ that is very similar to the one constructed for exciting KBOs. $p(v, n, d)$ is equal to the number of times n KBOs have an eccentricity greater than 1.0 in distance bin d with velocity v divided by the product of the total number of runs at velocity v and forty. We then calculate $\langle\sigma\rangle_d$ in the same manner as the excited KBOs (equation 3.2) and then calculate the probability of losing x KBOs (equation 3.3).

Comparing the data in Fig. 3.8 to the data in Fig. 3.7, we see that in all cases, the probability to lose KBO is just slightly smaller than the probability to excite the KBOs. Even further, to have disk truncation, we would expect to see that a majority of the KBOs in the outer distance bins would be lost while having a low probability within the inner distance bins. What we see is that at the outer bins, there is a chance of losing 5% of the KBOs and exciting another 5%, but the probability for affecting a large fraction of the KBOs is small. The probability of losing 50% in the any bin is practically zero. We will note that our simulation is set up such that we assume that the KBO's eccentricity is zero before any close encounter. Thus, if our Solar System is in a region in which we would expect to see multiple close encounters (Fig. 3.1), the effects of a close encounter on a previously excited KBO is not taken into account in our simulation.

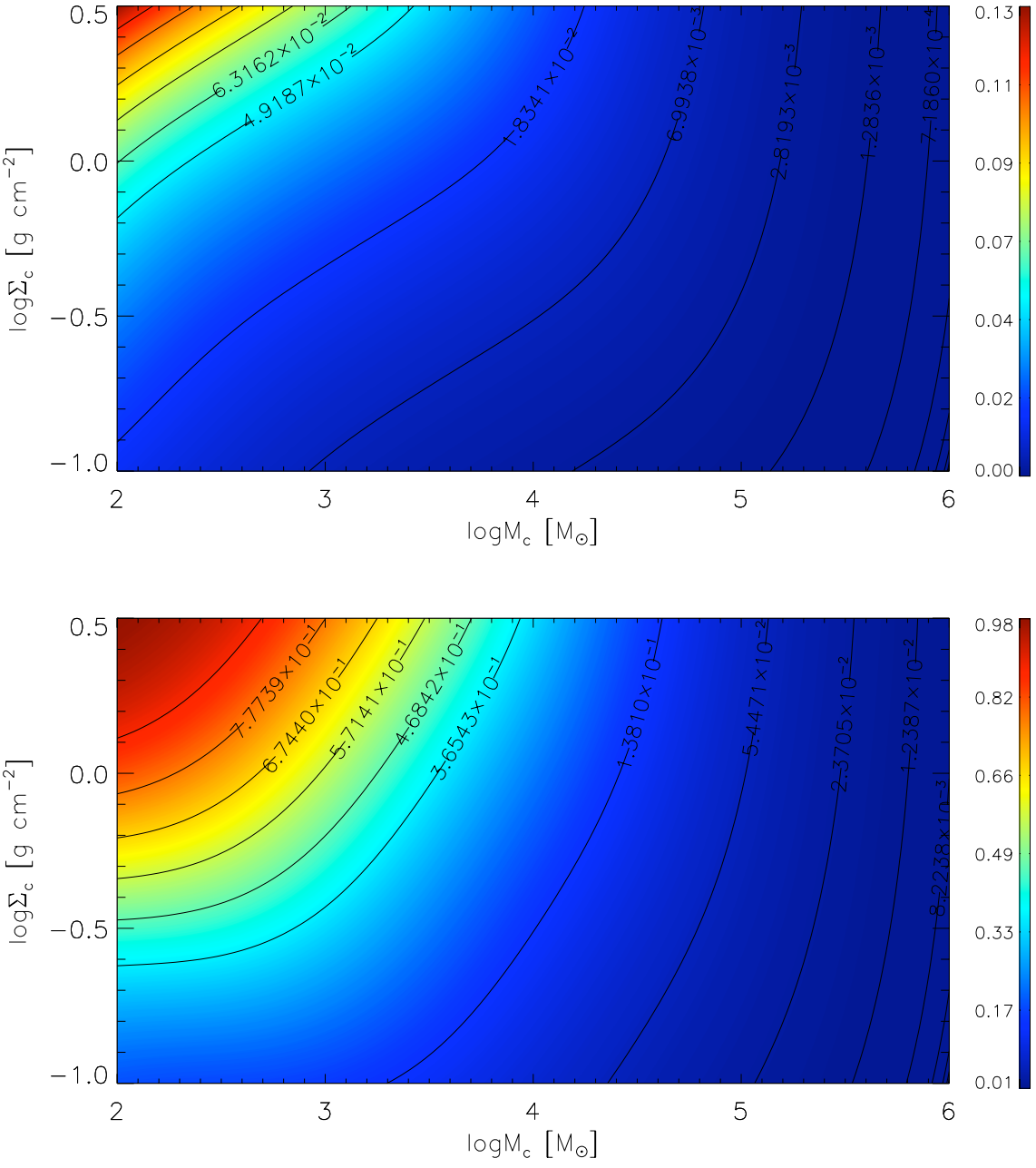

Figure 3.7: The probability of exciting one KBO in the distance range of 35 AU to 80 AU (panel a) and in the distance range of 455 AU to 500 AU (panel b).

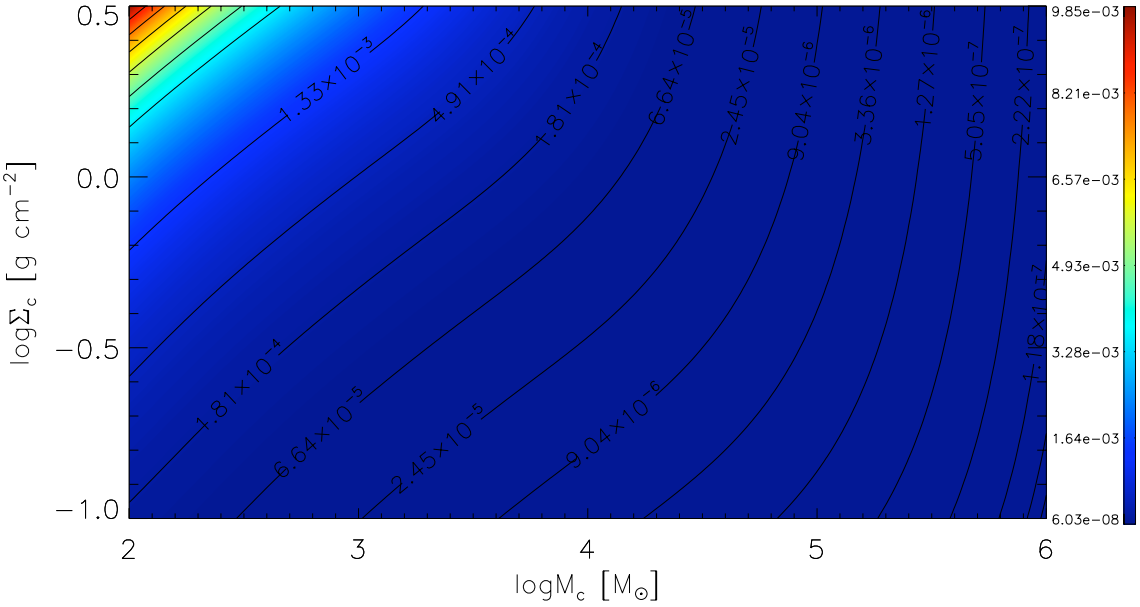

(a) Lost 5% with d=35-80 AU

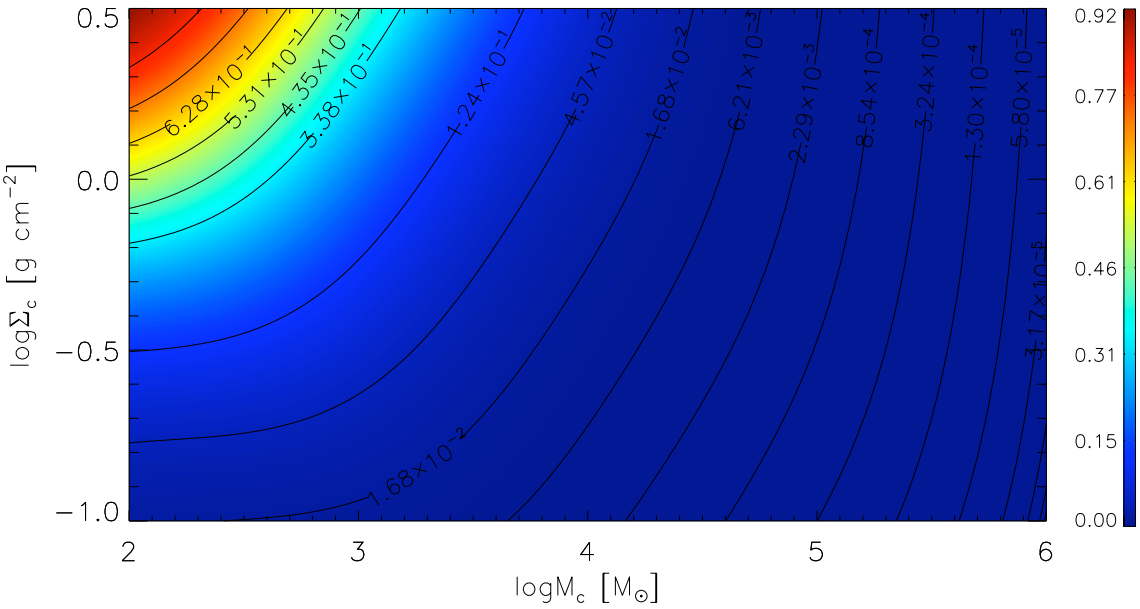

(b) Lost 5% with d=455-500AU

Figure 3.8

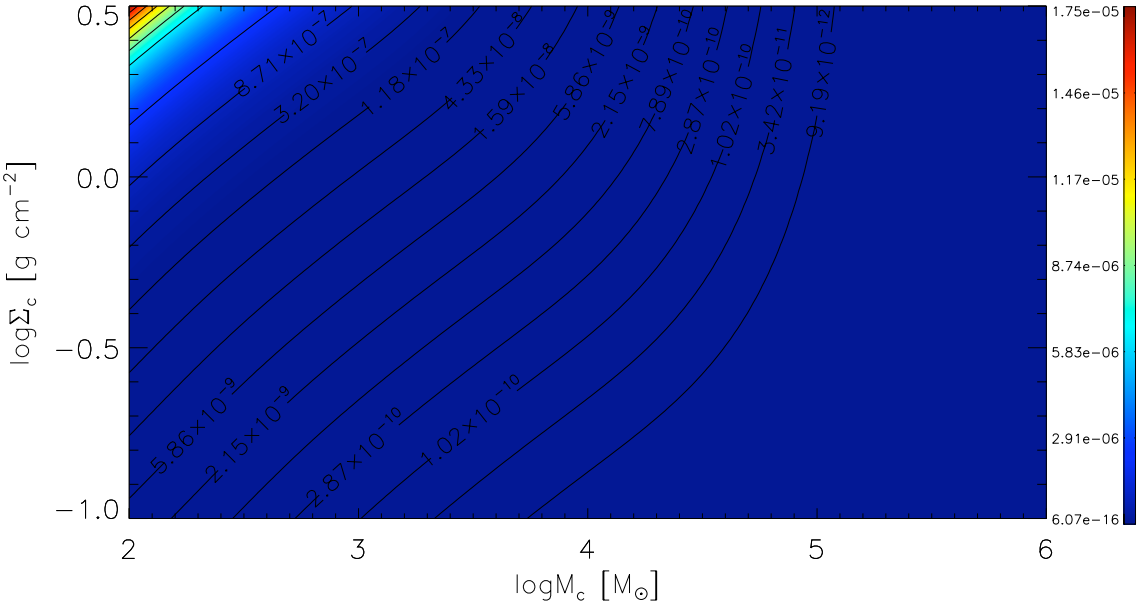

(c) Lost 10% with d=35-80 AU

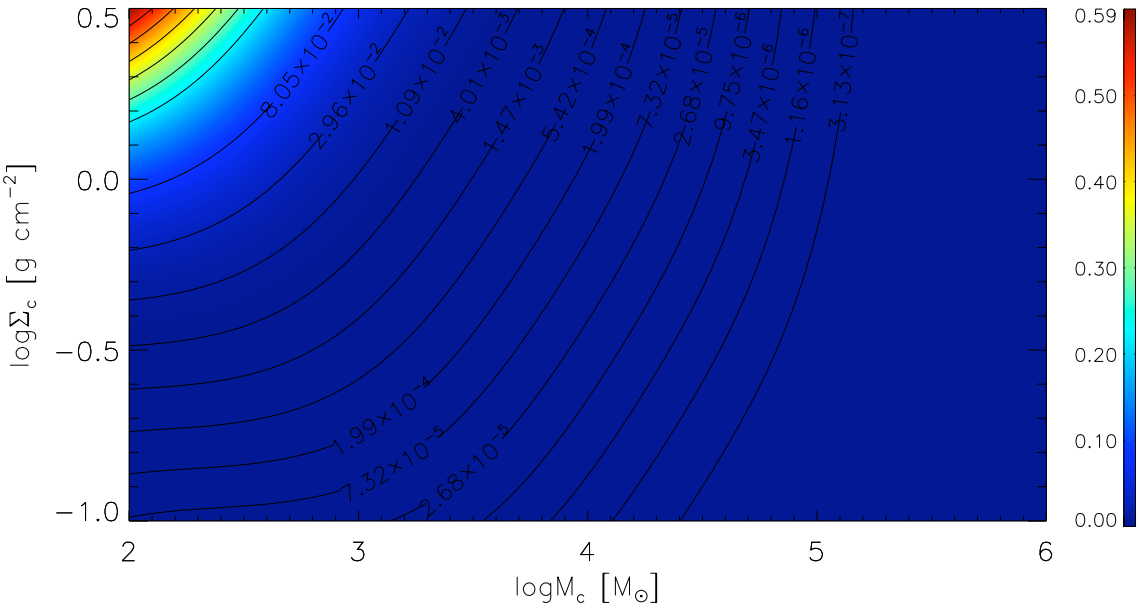

(d) Lost 10% with d=455-500AU

Figure 3.8

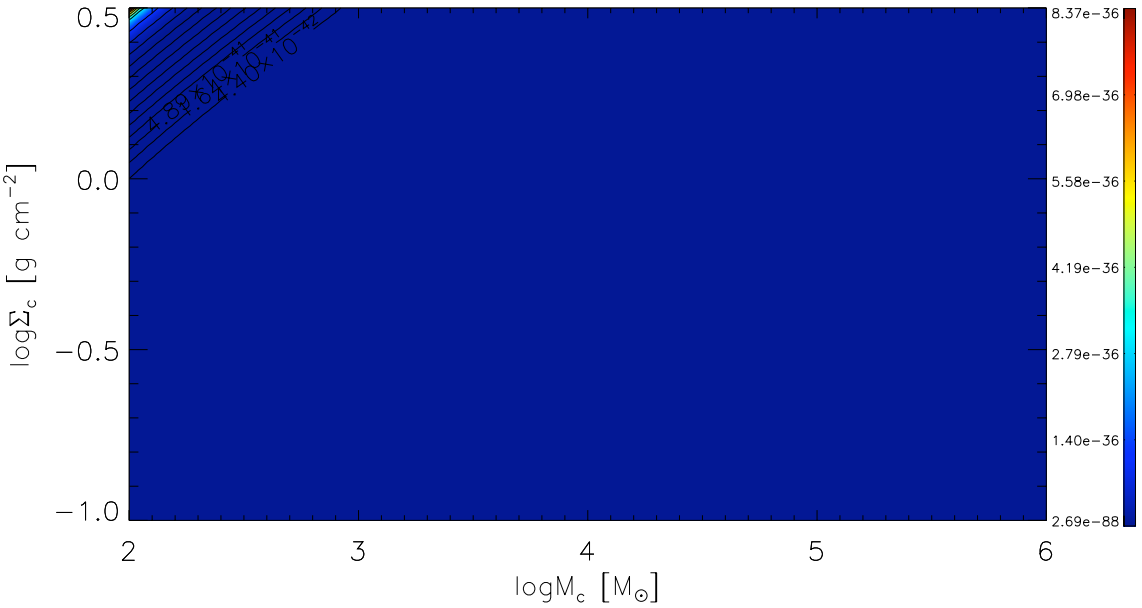

(e) Lost 50% with d=35-80 AU

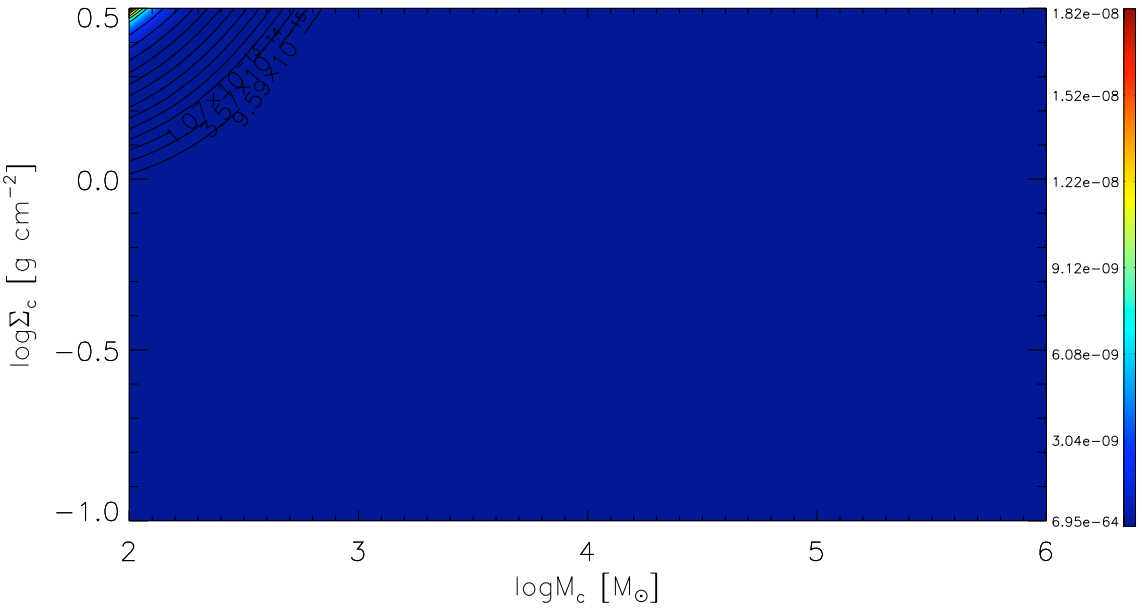

(f) Lost 50% with d=455-500AU

Figure 3.8: This shows the probability that, in one crossing time, 5% (a and b), 10% (c and d) and 50% (e and f) of the KBOs in distance bin d will become unbound as a function of $\log M_c$ and $\log \Sigma_c$. In all cases, the inner bin and the outer bin where the extreme values.

3.3 Effects of Close Encounters on Nemesis

Finally, we would like to address the question, could Nemesis survive the birth cluster? To answer this we began with $\langle\sigma\rangle_{Nem}$ which is constructed in a similar fashion as the Jovian planets. From $\langle\sigma\rangle_{Nem}$, we calculate Λ_{Nem} and P_{Nem} and plot the results in Figs. 3.9 and 3.10.

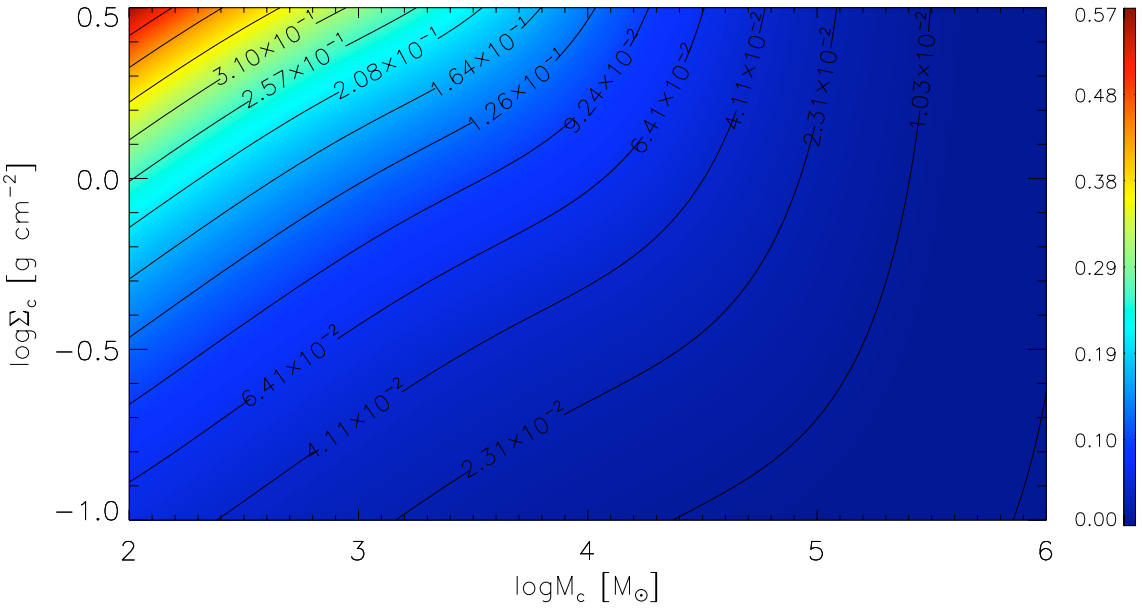

Figure 3.9: Expected number of encounters per crossing time that will result in Nemesis becoming unbound from the Sun, as a function of $\log M_c$ and $\log \Sigma_c$. As we can see, the expected number of encounters is < 1 at all values of M_c and Σ_c.

As shown in Fig. 3.9, although the number of encounters that will cause Nemesis to become unbound is greater than the number expected to excite Jovian planet eccentricities, the expected number is still < 1 in all cases of surface density and cluster mass. Furthermore, the probability of Nemesis becoming unbound, shown in Fig 3.10, shows that stripping remains unlikely unless the cluster is small and dense.

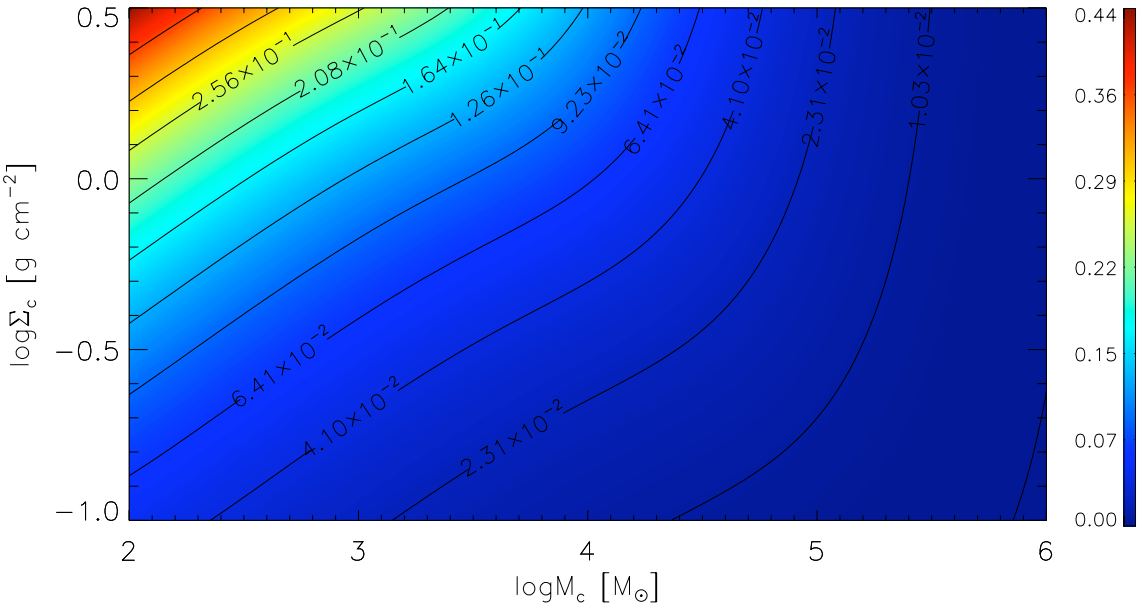

Figure 3.10: Probability that, in one crossing time, Nemesis will become unbound, as a function of $\log M_c$ and $\log \Sigma_c$. The probability of losing Nemesis is low except in low mass high density clusters.

4 Conclusion

Adams (2010) argues for a lower bound of the birth cluster membership size based of meteorite evidence and the upper bound based on estimates of the effects of cluster dynamics on the Solar Nebula. The meteorite evidence suggests that a supernova deposited short lived radioactive isotopes near the forming Solar System. However, the probability of having a supernova within the range needed is only about 2% for Adam's upper bound of the birth cluster membership size, $\sim 10^4$ stars. Adams determined this limit based on his estimate that above this size that the density of stars would have been so great as to guarantee an encounter with the impact parameter of 225 AU, thus disrupting the eccentricities of the Jovian planets.

Our data suggest that as the mass of the birth cluster increases, the relative velocities of the constituents increases and the effective impact parameters for Solar System-disrupting events decreases. Given this knowledge, high mass birth clusters are less likely to disrupt the Solar Nebula, and thus using cluster dynamics to determine an upper bound on the birth cluster's membership size would be in error. Figures 3.4 and 3.5 shows that the as the cluster mass increases, the expected number of encounters and the probability decreases, yet the number of encounters within an impact parameter of 2000 AU is independent of cluster mass. As cluster mass increases, the relative velocity increases but the number of encounters does not, and therefore there will be less interaction time between our Solar System and other stars within the cluster.

Given this, we feel we can remove the upper bounds to the membership size proposed by Adams (2010) and suggest that cluster dynamics play a minimal role in the formation of the Solar

System. The removal of the upper bounds then allows us the cluster size to be large enough to be able to produce massive star which can go supernova to seed the Solar System with the observed short lived radioactive isotopes. With the upper bounds lifted, multiple supernovas can then be used to seed the Solar Nebula, thus allowing the supernovas to be further away and exposing the Solar System to less mass loss.

A close encounter within the birth cluster has also been proposed explain the existence of Sedna (See Section 1). We have looked into the probability of exciting a KBO from an eccentricity of zero to one between 0.5 and 1.0 (See Section 3.2.1). These results (shown in Fig. 3.7) show that the chances for exciting at least 5% of the KBOs with initial semi-major axis of 35-80 AU is less than 1%. However the probability of exciting at least 5% of the KBOs within the distance of 455-500 AU is ∼75% at the low mass, high surface density extreme, but quickly falls to less than 1% in intermediate mass clusters. This shows that producing a Sedna-like object is favored in the low mass and higher density clusters. However, it is unlikely that Sedna was produced in a close encounter in the mass range where a supernova is likely to happen.

We also looked into the concept of a close encounter stripping off outer KBOs to explain to the sudden density drop in KBO objects at 45 AU (See Section 1). Again, our data shows that in the low mass, high surface density extreme, there is a reasonable chance of losing at least 5% of the KBOs in the outer distance bin, but less than 1% chance of losing at least 5% of the KBOs in the inner distance. However, the probability of losing half of the KBOs in the outer distance bin on the order of 10^{-12}, even for the low mass, high surface density extreme case that is most favorable for stripping. This clearly shows that it is highly unlikely for a close encounter to truncate the Kuiper Belt.

The effects of cluster dynamics on the existence of Nemesis is inconclusive. The probability of losing Nemesis in low mass, high surface density clusters $\sim 32\%$, but for all other situations the probability is $< 10\%$. Given that we placed Nemesis at 1000 AU, far below the theorized semi-major axis of 33,000 AU to 88,000 AU, the probability of losing Nemesis should increase as Nemesis

becomes further from the Sun, and thus we can make no conclusion as to the viability of Nemesis within the birth cluster.

Bibliography

Adams, F. C. 2010. The birth environment of the solar system. *Annu. Rev. Astron. Astrophys.*, 48:47–85.

Allen, R. L., Bernstien, G. M., and Malhotra, R. 2001. The edge of the solar system. *ApJ*, 549:L241.

Carroll, B. and Ostlie, D. 2007. *An Introduction to Modern Astrophysics*. Addison-Wesley, 2nd edition.

Chabrier, G. 2005. The initial mass function : From salpeter 1955 to 2005. In Corbelli, E., Palla, F., and Zinnecker, H., editors, *The Initial Mass Function 50 Years Later*, volume 327 of *Astrophysics and Space Science Library*.

Chandar, R., Fall, S. M., and Whitmore, B. C. 2010. New test for disruption mechanisms of star clusters: The large and small magellanic clouds. *ApJ*, 711:1263–1279.

Davis, M., Hut, P., and Muller, R. A. 1984. Extinction of species by periodic comet showers. *Nature*, 308:715–717.

Duquennoy, A. and Mayor, M. 1991. Multiplicity among solar-type stars in the solar neighbourhood. *A&A*, 248:485–524.

Kouwenhoven, M. B. N., Brown, A. G. A., Zwart, S. F. P., and Kaper, L. 2007. The primordial binary population. ii. recovering the binary population for intermediate mass stars in scorpius ob2. *A&A*, 474:77–104.

Kroupa, P. 2002. The initial mass function and its variation. *ASP Conference Series*, 285:86–93.

Lada, C. J. 2006. Stellar multiplicity and the initial mass function: Most stars are single. *ApJ*, 640L:L63.

Lada, C. J. and Lada, E. A. 2003. Embedded clusters inmolecular clouds. *Annu. Rev. Astron. Astrophys.*, 41:57–115.

Press, W. H., Teukolsky, S. A., Vetterling, W. T., and Flannery, B. P. 1988. *Numerical Recipes in C*. The Press Syndicate of the University of Cambridge, 2nd edition.

Raup, D. M. and Sepkoski Jr., J. J. 1984. Periodicity of extinctions in the geologic past. *Proc. Natl. Acad. Sci.*, 81:801–805.

Schwamb, M. E. and et al. 2010. Properties of the distant kuiper belt: Results from the palomar distant solar system survey. *ApJ*, 720:1691–1707.

Tan, J. C. and et al. 2006. Equilibrium star cluster formation. *ApJ*, 641:L121.

Tohline, J. 2002. The origin of binary stars. *Annu. Rev. Astron. Astrophys.*, 40:349–385.

Whitmire, D. P. and Jackson IV, A. A. 1984. Are periodic mass extinctions driven by a distant solar companion? *Nature*, 308:713–715.